AIP | Applied Physics Letters

Nonthermal plasma synthesis of size-controlled, monodisperse, freestanding germanium nanocrystals

Ryan Gresback, Zachary Holman, and Uwe Kortshagen

Citation: Applied Physics Letters **91**, 093119 (2007); doi: 10.1063/1.2778356
View online: http://dx.doi.org/10.1063/1.2778356
View Table of Contents: http://scitation.aip.org/content/aip/journal/apl/91/9?ver=pdfcov
Published by the AIP Publishing

APPLIED PHYSICS LETTERS **91**, 093119 (2007)

Nonthermal plasma synthesis of size-controlled, monodisperse, freestanding germanium nanocrystals

Ryan Gresback, Zachary Holman, and Uwe Kortshagen[a]
Department of Mechanical Engineering, University of Minnesota, 111 Church St. SE, Minneapolis, Minnesota 55455

(Received 30 April 2007; accepted 9 August 2007; published online 29 August 2007)

Germanium nanocrystals may be of interest for a variety of electronic and optoelectronic applications including photovoltaics, primarily due to the tunability of their band gap from the infrared into the visible range of the spectrum. This letter discusses the synthesis of monodisperse germanium nanocrystals via a nonthermal plasma approach which allows for precise control of the nanocrystal size. Germanium crystals are synthesized from germanium tetrachloride and hydrogen entrained in an argon background gas. The crystal size can be varied between 4 and 50 nm by changing the residence times of crystals in the plasma between ~30 and 440 ms. Adjusting the plasma power enables one to synthesize fully amorphous or fully crystalline particles with otherwise similar properties. © *2007 American Institute of Physics*. [DOI: 10.1063/1.2778356]

Semiconductor nanocrystals have received significant attention in recent years due to their size-dependent optical and electronic properties. Most of the attention given to group IV semiconductor nanocrystals has focused on silicon nanocrystals (Si-NCs), due to their efficient and tunable light emission.[1–5] However, germanium nanocrystals (Ge-NCs) may be more interesting than Si-NCs for device applications that require a small band gap material, a material that exhibits stronger quantum confinement than Si, or a material that absorbs light better than Si. In particular, Ge-NCs may be well suited for photovoltaic applications since both theoretical[6,7] and experimental[8] studies have shown that the band gap of Ge-NCs can be tuned across the solar spectrum from the bulk Ge band gap of ~0.7 eV to ~2 eV for crystals 3 nm in diameter.

Many Ge-NC synthesis techniques have previously been reported. Liquid-phase Ge-NC synthesis[8–12] techniques are convenient for subsequent liquid-phase surface-functionalization reactions, but these synthetic routes are often time consuming, have low material yields, and sometimes produce Ge-NCs with broad size and shape distributions. Ge-NCs can also be precipitated in the solid phase,[13–16] which leaves Ge-NCs embedded in a matrix material that, in many cases, passivates the surfaces very well. However, the range of possible surface treatments for embedded Ge-NCs is limited, as is the flexibility of using embedded NCs for device applications. Gas-phase synthesis[17] produces freestanding Ge-NCs, whose surfaces are easily accessible for functionalization.[5,18,19] Unfortunately, uncontrollable particle agglomeration is present in most gas-phase processes. Such agglomeration makes it challenging to synthesize NCs with a narrow size distribution and may cause loss of quantum confinement.[20]

Previously, we reported a nonthermal plasma technique with large material yields for the synthesis of freestanding Si-NCs.[21] In this letter, we describe the adaptation of this synthetic approach to the synthesis of nearly monodisperse, freestanding Ge nanoparticles which can be produced to be either crystalline or amorphous, and whose mean diameter can be controlled from 4 to 50 nm.

A flow-through, nonthermal plasma reactor similar to that described in Ref. 21 was used to synthesize Ge-NCs. As sketched in Fig. 1, the reactor consists of a 25 mm outer diameter quartz tube through which precursor gases are passed. A Radio frequency power of 50–90 W at 13.56 MHz is applied to a ring electrode pair wrapped around the tube, resulting in an ~5 cm long plasma that causes precursor dissociation and subsequent NC formation. The NCs are collected downstream of the plasma on transmission electron microscope (TEM) grids or stainless steel filter meshes.

Germanium tetrachloride ($GeCl_4$) entrained in an argon (Ar) buffer is used as the Ge-NC precursor. Ar is bubbled through a $GeCl_4$-containing bubbler which is held at 200 kPa so that the gas mixture entering the reactor has a $GeCl_4$:Ar ratio of 5:95. Hydrogen (H_2) and additional Ar are also added to the gas flow entering the reactor; H_2 serves to scavenge chlorine (Cl) produced in the dissociation of $GeCl_4$, while Ar acts as a background gas in the plasma and can be adjusted to alter the total gas flow rate. The operating pressure in the plasma reactor is ~266 Pa.

The NC residence time in the plasma zone is the primary parameter affecting NC size, with longer times leading to larger particles. Figure 2 shows TEM images of Ge-NCs collected on TEM grids downstream of the plasma for 1 min.

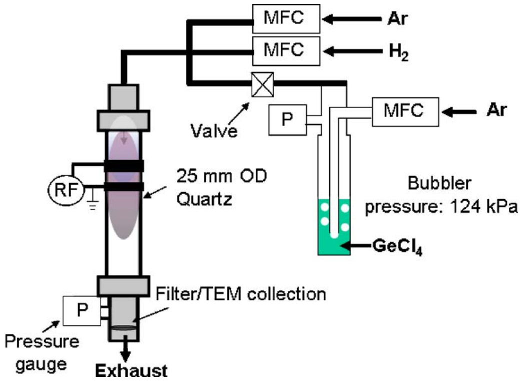

FIG. 1. (Color online) Schematic of the experimental setup.

---

[a] Electronic mail: uk@me.umn.edu

0003-6951/2007/91(9)/093119/3/$23.00

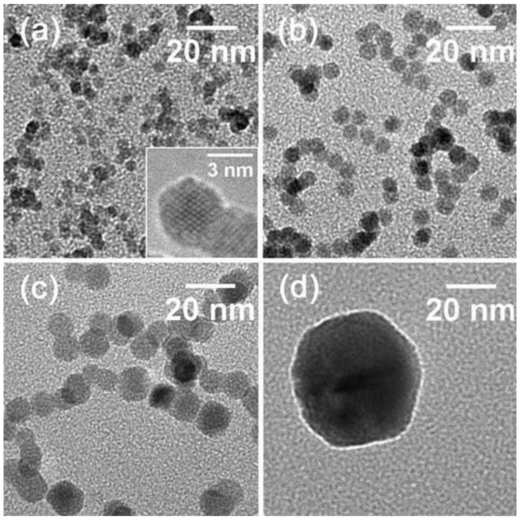

FIG. 2. Plasma synthesized germanium nanocrystals for various residence times in the plasma. Precursor flow rates were (a) 110 SCCM Ar, 10 SCCM H_2, and 0.5 SCCM $GeCl_4$ (inset shows high resolution); (b) 55 SCCM Ar, 5 SCCM H_2, and 0.25 SCCM $GeCl_4$; (c) 27.5 SCCM Ar, 2.5 SCCM H_2, and 0.13 SCCM $GeCl_4$; and (d) 6.9 SCCM Ar, 0.63 H_2, and 0.03 SCCM $GeCl_4$. All depositions were for ~1 min at 80 W power.

The $Ar:H_2:GeCl_4$ gas flow ratio was held constant at 220:20:1 while the total flow rate was varied from 121 to 7.5 SCCM (SCCM denotes cubic centimeter per minute at STP), and thus the residence time from ~27 to ~440 ms. It is clearly seen that the Ge-NCs are rather monodisperse under all conditions and that longer residence times lead to larger crystals. The effect of residence time on NC size is quantitatively summarized in Fig. 3. The mean particle diameter changes by about a factor of 10 when the residence time is adjusted throughout the above range, indicating the versatility of this synthesis technique. The smallest NC size achieved is ~3 nm. According to theoretical calculations by Nesher *et al.*[7] and Takagahara and Takeda,[6] and absorption measurements by Wilcoxon *et al.*,[8] 3 nm Ge-NCs are predicted to have a band gap of ~2 eV. Based on these studies, it is expected that the band gap of the produced Ge-NCs can be smoothly varied from the bulk Ge band gap of ~0.7 eV (for large NCs) to ~2 eV (for 3 nm NCs) by altering the NC residence time in the plasma.

Compared to Ge-NCs synthesized using many of the techniques previously reported in the literature, the size and shape distributions of our particles are rather narrow, though the distributions broaden with increasing particle size (Fig. 3). For 5 nm Ge-NCs, standard deviations (determined by measurement of >50 NCs from TEM images) of 10%–15% are typical. The particles are nearly uniformly spherical at small sizes, but some shape deviations are introduced at larger sizes and faceting can be seen. In addition, the particles do not fuse together to form "hard" agglomerates. Rather, the boundaries between particles are easily distinguishable and, as we will show in a different paper, NCs that may appear to be "stuck together" are easily separated during liquid-phase chemical reactions used to terminate the NC surfaces. As we previously reported for Si-NCs,[21] we believe that the plasma environment effectively inhibits agglomeration by dispensing a unipolar negative charge on the NCs. Nonagglomerated, monodisperse particles such as the Ge-NCs reported here are required for many device processing steps such as the formation of densely packed or superlattice films from NC colloidal solutions.[22,23]

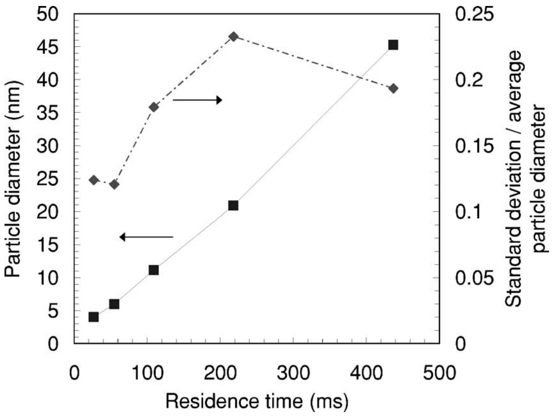

FIG. 3. Particle mean diameter and standard deviation of the particle size distribution as a function of the particle residence time in the reactor. Plasma conditions were as in Fig. 2.

Gas flow ratios other than 220:20:1 $Ar:H_2:GeCl_4$ may be used to alter NC production. In particular, simultaneously increasing the $GeCl_4$ and H_2 flows results in greater mass yield—with yields as high as tens of milligrams per hour—but does not significantly affect the NC size since the much larger Ar flow is the dominant factor in determining the residence time. Changing the $GeCl_4:H_2$ ratio alters both the NC size and yield, with more H_2 leading to larger Ge-NCs and too little H_2 resulting in no NC formation. We believe that H radicals prevent the fast recombination of Cl with fragments of dissociated $GeCl_4$ so that $GeCl_4$ fragments have a chance to bond with each other, leading to Ge-NC nucleation. We suspect that, in the absence of H_2 gas, Cl radicals reattach to Ge atoms to re-form $GeCl_4$ before Ge-NC nucleation can occur. With increasing H_2, less Cl is present to hinder Ge-NC growth, leading to larger particles. For practical purposes, it is convenient to fix the $GeCl_4:H_2$ ratio and alter only the parameters already discussed, since these give more than adequate control of the NC size and mass yield.

The amount of power coupled to the plasma provides an effective handle on the particle crystallinity without altering the particle size or mass yield. Figure 4 compares x-ray diffraction (XRD) and TEM results for samples grown with 60 and 90 W power, and otherwise identical conditions. Two broad features characteristic of amorphous material are seen in the XRD pattern of the low power sample, while the (111), (220), (311), (400), and (331) diffraction peaks of diamond cubic Ge are clearly visible for the high power sample. The width of the diffraction peaks is consistent with the Ge-NC size of ~5 nm observed in TEM. Selected-area diffraction (SAD) performed in the TEM corroborates these results; rings corresponding to the (111), (220), and (311) diffractions are present in the SAD pattern of the high power sample but not the low power sample. Crystallinity aside, Ge nanoparticles synthesized with 60 and 90 W are similar in both their shape and size, as seen in the TEM images shown in Fig. 4.

While crystalline materials are generally preferred for their superior electronic properties, certain applications may favor amorphous materials and it is convenient to be able to easily synthesize both crystalline and amorphous Ge nanoparticles. For example, a nanoporous polycrystal could be made by depositing a few crystalline NC seeds in a porous film of amorphous Ge particles so that, upon annealing, the

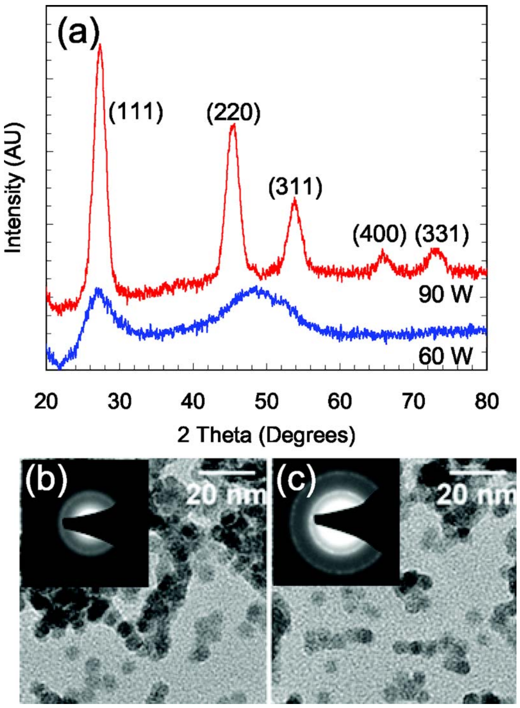

FIG. 4. (Color online) (a) X-ray diffraction patterns of particles synthesized with 60 and 90 W power. Both samples were deposited for 20 min using 60 SCCM Ar, 15 SCCM H_2, and 0.5 SCCM $GeCl_4$. Transmission electron micrographs and selected area diffraction patterns of particles deposited for 1 min with the above flow rates using (b) 60 W and (c) 90 W power.

amorphous particles adopt the crystallographic orientation of the NC seeds to form extended, porous crystals.

Nanocrystalline Ge with feature sizes smaller than ~6 nm have been reported by others to exhibit visible photoluminescence (PL).[8,24–29] The source of this PL is controversial, with some authors claiming that it is intrinsic to the NCs and is blueshifted due to quantum confinement,[8,24,25] and others claiming it to be extrinsic and resulting from oxides and defects.[26–29] No PL was observed from the Ge-NCs reported here, independent of their size and oxidation state. This may possibly be a result of Cl on the NC surfaces, since halogens have been observed to quench PL in porous Si.[30]

In summary, we have demonstrated the synthesis of freestanding Ge-NCs using a nonthermal plasma technique which allows control of the NC properties. Nearly monodisperse NCs with mean diameters of 4–50 nm have been synthesized with mass yields as high as tens of milligrams per hour. The nanoparticle crystallinity can be controlled independent of other particle properties by varying the plasma power. As the plasma synthesis approach produces Ge-NCs without any surfactants, subsequent surface functionalization schemes can likely be used to impart additional functionality to the particles.

This work was supported primarily by the MRSEC Program of the National Science Foundation under Award No. DMR-0212302 and by the Initiative for Renewable Energy and the Environment under Grant No. LG-C5-2005. Partial support was also provided by NSF-IGERT Grant No. DGE-0114372.

[1] A. G. Cullis and L. T. Canham, Nature (London) **335**, 335 (1991).
[2] J. P. Wilcoxon, G. A. Samara, and P. N. Provencio, Phys. Rev. B **60**, 2704 (1999).
[3] J. D. Holmes, K. J. Ziegler, C. Doty, L. E. Pell, K. P. Johnston, and B. A. Korgel, J. Am. Chem. Soc. **123**, 3743 (2001).
[4] X. Li, Y. He, S. S. Talukdar, and M. T. Swihart, Langmuir **19**, 8490 (2003).
[5] D. Jurbergs, L. Mangolini, E. Rogojina, and U. Kortshagen, Appl. Phys. Lett. **88**, 233116 (2006).
[6] T. Takagahara and K. Takeda, Phys. Rev. B **46**, 15578 (1992).
[7] G. Nesher, L. Kronik, and J. R. Chelikowsky, Phys. Rev. B **71**, 035344 (2005).
[8] J. P. Wilcoxon, P. P. Provencio, and G. A. Samara, Phys. Rev. B **64**, 035417 (2001).
[9] J. R. Heath, J. J. Shiang, and A. P. Alivisatos, J. Phys. Chem. **101**, 1607 (1994).
[10] B. R. Taylor, S. M. Kauzlarich, H. W. H. Lee, and G. R. Delgardo, Chem. Mater. **10**, 22 (1998).
[11] D. Gerion, N. Zaitseva, C. Saw, M. F. Casula, S. Fakra, T. Van Buuren, and G. Galli, Nano Lett. **4**, 597 (2004).
[12] X. Lu, B. A. Korgel, and K. P. Johnston, Chem. Mater. **17**, 6479 (2005).
[13] M. Fujii, S. Hayashi, and K. Yamamoto, Jpn. J. Appl. Phys., Part 1 **30**, 687 (1991).
[14] J. G. Zhu, C. W. White, J. D. Budai, S. P. Withrow, and Y. Chen, J. Appl. Phys. **78**, 4386 (1995).
[15] W. K. Choi, H. G. Chew, V. Ho, V. Ng, W. K. Chim, Y. W. Ho, and S. P. Ng, J. Cryst. Growth **288**, 79 (2006).
[16] T. P. L. Pederson, J. S. Jensen, J. Chevallier, O. Hansen, J. M. Jensen, B. B. Nielsen, and A. N. Larsen, Appl. Phys. A: Mater. Sci. Process. **81**, 1591 (2005).
[17] C. Bostedt, T. van Buuren, J. M. Plitzko, T. Möller, and L. J. Terminello, J. Phys.: Condens. Matter **15**, 1017 (2003).
[18] Y.-C. Liao and J. T. Roberts, J. Am. Chem. Soc. **128**, 9061 (2006).
[19] A. M. Nienow and J. T. Roberts, Chem. Mater. **18**, 5571 (2006).
[20] C. Bostedt, T. van Buuren, T. M. Willey, and L. J. Terminello, Appl. Phys. Lett. **85**, 5334 (2004).
[21] L. Mangolini, E. Thimsen, and U. Kortshagen, Nano Lett. **5**, 655 (2005).
[22] C. P. Collier, T. Vossmeyer, and J. R. Heath, Annu. Rev. Phys. Chem. **49**, 371 (1998).
[23] C. B. Murray, C. R. Kagan, and M. G. Bawendi, Annu. Rev. Mater. Sci. **30**, 545 (2000).
[24] Y. Maeda, Phys. Rev. B **51**, 1658 (1995).
[25] B. R. Taylor, S. M. Kauzlarich, G. R. Delgardo, and H. W. H. Lee, Chem. Mater. **11**, 2493 (1999).
[26] S. Miyazaki, K. Sakamoto, K. Shiba, and M. Hirose, Thin Solid Films **255**, 99 (1995).
[27] M. Zacharias and P. M. Fauchet, Appl. Phys. Lett. **71**, 380 (1997).
[28] G. Kartopu, S. C. Bayliss, V. A. Karavanskii, R. J. Curry, R. Turan, and A. V. Sapelkin, J. Lumin. **101**, 275 (2003).
[29] H. P. Wu, M. Y. Ge, C. W. Yao, Y. W. Wang, Y. W. Zeng, L. N. Wang, G. Q. Zhang, and J. Z. Jiang, Nanotechnology **17**, 5339 (2006).
[30] J. M. Buriak, Chem. Rev. (Washington, D.C.) **102**, 1271 (2002).